


## Article

# Overlay Optimization Algorithm for Directed Sensor Networks with Virtual Force and Particle Swarm Optimization Synergy

Lingjian Zhu <sup>1,\*</sup> , Li Lin <sup>1</sup>, Qi Liang <sup>2</sup>, Yaling Lu <sup>3</sup>, Haonan Tan <sup>1</sup>, Xuan Ma <sup>3</sup> and Dongya Zhang <sup>1</sup>

<sup>1</sup> School of Mechanical and Precision Instrument Engineering, Xi'an University of Technology, Xi'an 710048, China; 2230220140@stu.xaut.edu.cn (L.L.); 2210220121@stu.xaut.edu.cn (H.T.); dyzhang@xaut.edu.cn (D.Z.)

<sup>2</sup> Guangxi Research Institute of Metrology & Test, Nanning 530299, China; ivy2325\_cn@sina.com

<sup>3</sup> College of Automation, Xi'an University of Technology, Xi'an 710048, China; 2230220136@stu.xaut.edu.cn (Y.L.); maxuan@xaut.edu.cn (X.M.)

\* Correspondence: zlj\_zhy@xaut.edu.cn

**Abstract:** In this study, a novel algorithm for optimizing the coverage of directed sensor networks is proposed. The deployment of sensor networks is typically random, leading to the potential issues of extensive coverage overlaps and blind areas. To address this challenge and enhance the effectiveness of network coverage, a directional sensor network coverage optimization algorithm is developed based on the principles of virtual force and particle swarm optimization. Firstly, the article introduces the concept of a segmented virtual negative centroid model. This model revolutionizes the configuration of the virtual negative centroid, thereby enabling a more efficient adjustment of the gravitational forces exerted by the coverage blind areas on the sensor nodes. Therefore, the influence of these blind areas on the improvement of network coverage is significantly amplified. Secondly, taking into account the characteristics of global optimization and the inherent randomness of particle swarm optimization, the algorithm synergistically combines the principles of virtual force and particle swarm optimization. This integration effectively fine-tunes the sensing direction of the sensor nodes, thereby optimizing their overall performance. The algorithm in this study incorporates an adjusted inertia weight strategy and introduces Gaussian disturbance in the local optimization enhancement phase to prevent local optimization, accelerate particle convergence, and facilitate the sensor network's attainment of an optimal distribution for coverage optimization. Simulation experiments were conducted to verify the algorithm's effectiveness. The initial sensor network coverage was 31.04%. After applying the algorithm, the average coverage increased to 80.16%, with a maximum coverage of 84.2%. These results verify the effectiveness of the algorithm.

**Keywords:** directed sensor network; virtual force model; particle swarm optimization; coverage optimization



**Citation:** Zhu, L.; Lin, L.; Liang, Q.; Lu, Y.; Tan, H.; Ma, X.; Zhang, D. Overlay Optimization Algorithm for Directed Sensor Networks with Virtual Force and Particle Swarm Optimization Synergy. *Electronics* **2023**, *12*, 4332. <https://doi.org/10.3390/electronics12204332>

Academic Editor: Chrysostomos Stylios

Received: 12 September 2023

Revised: 13 October 2023

Accepted: 17 October 2023

Published: 19 October 2023



**Copyright:** © 2023 by the authors. Licensee MDPI, Basel, Switzerland. This article is an open access article distributed under the terms and conditions of the Creative Commons Attribution (CC BY) license (<https://creativecommons.org/licenses/by/4.0/>).

## 1. Introduction

A directional sensor network is composed of numerous directional sensor nodes possessing wireless communication and computing capabilities [1,2]. Through wireless communication, a multi-hop self-organizing network is established, facilitating information collection, transmission, and processing in the designated area. Sensors employing directional perception models, including video sensors, ultrasonic sensors, and infrared sensors, find extensive applications in various domains such as industry, agriculture, military defense, and intelligent transportation [3–6]. The network's efficacy in monitoring tasks relies on its effective coverage, which serves as a prerequisite. The degree of coverage directly reflects the sensor network's capacity to perceive the target, thus playing a crucial role.

The monitoring environment, which assumes a pivotal role in determining the quality of network services, has been the subject of extensive research aimed at enhancing the regional coverage of sensor networks. Scholars have delved into various algorithms

pertaining to sensor node mobility, sensing direction adjustment, and the integration of both aspects. The primary objective behind relocating sensor nodes is to minimize coverage blind spots and overlaps in the network by strategically adjusting their positions, thereby optimizing regional coverage [7–10]. By considering the adjustability of sensor sensing directions, the movement and adjustment of sensor nodes are harmoniously combined to collectively optimize the distribution of sensor nodes in the network, thus yielding optimal results [11–14]. It is worth noting, however, that the integration of sensor node movement and sensing direction adjustment holds the potential to maximize network coverage in theory. Nevertheless, the mobility of sensor nodes necessitates the utilization of energy-intensive motors, resulting in exorbitant application costs.

At present, considerable attention is being devoted by numerous researchers to the investigation of algorithms that can effectively adjust the sensing direction of directional sensors. The authors of [15] employed the virtual force model in conjunction with the particle swarm optimization algorithm. By utilizing the virtual force as a perturbation factor to guide the evolution of the particle swarm, they achieved remarkable results in addressing the coverage optimization problem in directional sensor networks. Reference [16] proposed a multi-objective optimization model aimed at enhancing network coverage and reducing the redundancy rate of sensor nodes through the optimization of their sensing direction. Conversely, in reference [17], the directed covering model was transformed into a time covering model. By employing an integer linear programming optimization problem and local information, the authors successfully obtained the optimal solution for the time series covering problem. In addition, reference [18] focused on optimizing two objectives in directed sensor networks, namely the presence of redundant sensor nodes and network energy consumption. When optimizing the effective coverage in directed sensor networks, the objective is to maximize network coverage while minimizing the number of sensors and energy consumption. In the pursuit of addressing the coverage optimization problem in directional sensor networks, the deployment method of randomly throwing aircraft is commonly employed to initially establish sensor nodes in the network. During the deployment of sensor nodes, consideration must be given to the number of sensors in order to strike a balance that ensures the network operates efficiently. Insufficient initial sensor deployment may result in incomplete coverage of the target area, leading to data insufficiency or disruptions in operations. Conversely, an excessive number of sensors may result in unnecessary costs due to excessive network coverage. At present, the predominant focus in the advanced sensor optimization algorithms lies in the optimization of sensor network coverage based on a Voronoi diagram [19], as well as the implementation of an efficient Bayesian sensor placement algorithm for structural identification [20]. The Voronoi diagram-based approach facilitates the decentralized optimization of local coverage within each individual cell. On the other hand, the Bayesian sensor placement algorithm serves to circumvent potential issues of unrecognizability that may arise during the sequential process.

Despite the achievement of favorable coverage optimization results in the research on directional sensor networks, the fixed positioning of nodes imposes significant limitations on the service performance of sensor networks, as nodes are unable to move in the network.

In this paper, a novel approach, namely the segmented virtual negative centroid model, is proposed to enhance the gravity of coverage. This is achieved by strategically placing the virtual negative centroid in the blind areas of coverage and employing a combination of virtual force and particle swarm optimization to effectively adjust the sensing direction of the sensor nodes. By improving the inertia weight of the particle swarm optimization and introducing Gaussian disturbance to the particle swarm updating mechanism, the efficiency of the optimization process is significantly enhanced. This prevents premature convergence and enables the particles to promptly detect the optimal distribution of node perception direction in the network, thereby mitigating coverage overlap and blind spots.

This paper seeks to introduce the segmentation virtual negative centroid model, explain the improvements made, and discuss the adjustments made to the sensing direction

of the sensor nodes. In addition, the inertia weight strategy in the algorithm is fine-tuned to expedite the attainment of the optimal distribution in the sensor network, thereby facilitating coverage optimization.

## 2. Perception Model and Problem Description

### 2.1. Problem Hypothesis

With respect to the enhancement of regional coverage, this study optimizes the sensing direction of the sensor nodes to minimize both coverage overlap and blind areas. The following assumptions were made during the course of this research:

- (1) The positions of the sensor nodes remain fixed after their initial deployment.
- (2) All sensor nodes possess identical sensing radii and sensing angles.
- (3) Each sensor node is capable of acquiring its own position information and sensing direction, while also being able to obtain such information from other sensor nodes.

### 2.2. Direction Perception Model

The sensing area of a directed sensor node is a fan-shaped region centered around the sensor node, with the sensing radius as its radius. The schematic diagram is illustrated in Figure 1, where  $p$  represents the position of the sensor node,  $R$  represents the nodal perception radius and the nodal perception direction (from  $P$  to  $C$ ),  $\alpha$  represents half the sensing angle of the node, and  $2\alpha$  denotes the sensing angle of the sensing area of the sensor (when the sensing angle of the sensor is 0, the sensor is considered an omnidirectional sensing model),  $C$  denotes the position of the centroid of a node on the symmetry axis of the sector, and the distance from the center of the circle is  $\frac{2rs\sin\alpha}{3\alpha}$ . The centroid circle is divided into  $n$  parts, excluding the sensing sector, and each part's arc center point is considered a virtual negative centroid point. For instance,  $f_1, f_2, n$  represents the number of virtual negative centroids.

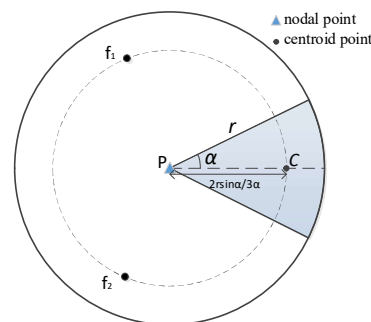


Figure 1. Direction perception model.

### 2.3. Direction Perception Model

The coverage rate, initially introduced by Gage [21,22], is defined as the ratio of the coverage area of all sensor nodes in the monitoring area to the total monitoring area. To simplify coverage calculation, this paper discretizes the continuous monitoring area and transforms the coverage calculation into the calculation of discrete points in the area. The target area is divided into intervals of  $\Delta x$  in both the horizontal and vertical directions, and discrete points are selected accordingly. If a discrete point in the region is covered by at least one sensor node, it is denoted as  $t^*$ , as depicted in Figure 2. Finally, according to the ratio of the total number of discrete points marked  $n$  to the total number of discrete points  $N$ , the coverage rate  $P$  of the monitoring area is calculated. The calculation formula is as follows:

$$P = \frac{\sum_{t=1}^n t^*}{N} \tag{1}$$

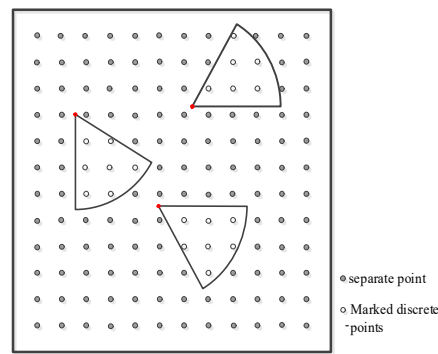


Figure 2. Covering model.

In the coverage calculation of sensor networks, discrete points are considered covered when they fall within the sensing area of nodes. For a discrete point to be covered, the following conditions must be met:

- (1)  $\left\| \vec{PP}_i \right\| \leq r$ ;  $\left\| \vec{PP}_i \right\|$  represents the modulus from  $P$  to  $P_i$  discrete points.
- (2) The range of values for the angle between  $\left\| \vec{PP}_i \right\|$  and  $\vec{V}(t)$  is  $[-\alpha, \alpha]$ .

Assuming that the number of sensor nodes in the monitoring area is  $n$ , the initial coverage rate is  $P_0$ , and the sensing direction of the  $i$ -th sensor is  $\vec{V}_i$ , the coverage optimization problem can be transformed into an optimization problem. The objective is to solve the optimal direction of a group of directional sensor nodes  $P(\vec{V}_1, \vec{V}_2, \dots, \vec{V}_n)$  and satisfy the following:

$$P(\vec{V}_1, \vec{V}_2, \dots, \vec{V}_n) \geq P_0 \tag{2}$$

### 3. Segment Virtual Negative Centroid Coverage Algorithm for Directed Sensor Networks

In light of the limitations in the existing references, a novel segmented virtual negative centroid model was devised in the framework of this study. The primary objective of this model was to rectify the gravitational inconsistencies arising from the blind area by enhancing the methodology employed for establishing the virtual negative centroid [23]. Subsequently, this model was integrated into the virtual force model to tackle the issue of directional sensor network coverage. Therefore, a segmented virtual negative centroid directional sensor network coverage algorithm was formulated to augment the network’s coverage.

#### 3.1. Split Virtual Negative Centroid Model

To explore the directed sensor network coverage, an algorithm predicated on the virtual potential field was introduced. This algorithm incorporated the force model of the virtual potential field into the study of directed sensor network coverage. In the virtual force model, the node’s sensing direction was guided towards the network’s blind area through the attractive force exerted by the virtual negative centroid on the sensor node. In this study, two virtual negative centroids were established in the blind area of the sensing circle through equal division. As the blind area in the sensing circle expanded, the attractive force generated by the two virtual negative centroids gradually weakened, thereby effecting minimal adjustments to the sensor nodes. Therefore, significantly enhancing the effective coverage of the sensor network posed a challenge.

In the current paper, the establishment of the virtual negative centroid was achieved through the equitable division of directional sensors, as depicted in Figure 3. Firstly, the perception angle of the node was evenly divided into  $n$  equal parts, and the angle of each equal part was set to  $\frac{2\alpha}{n}$ . The possible sensing area (except the node sensing area in the sensing circle) was segmented with an angle  $\frac{2\alpha}{n}$  as the segmentation benchmark, and a

virtual negative centroid was set at the centroid of each possible sensing area. Subsequently, a virtual negative centroid was positioned at the centroid of each potential sensing area. These virtual negative centroids exerted a virtual gravitational force on the sensor nodes, inducing their rotation towards the coverage blind area (i.e., the possible sensing area) and thereby enhancing the coverage of the sensor network. The number of “virtual negative centroids” that can be established in the sensing area of the sensor network is given by the following:

$$num = \frac{(360 - 2\alpha)}{2\alpha/n} \tag{3}$$

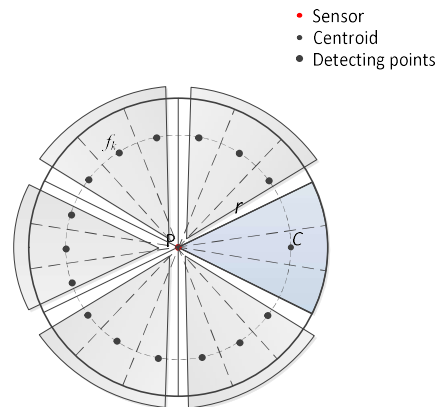


Figure 3. Split virtual negative centroid model.

### 3.2. Force Analysis

When the Euclidean distance between sensor node  $s_j$  and sensor node  $s_i$  (i.e., the distance between their respective centroid points) is less than twice the sensing radius of the sensor, they are considered neighboring nodes. As a result of the overlapping coverage areas between neighboring nodes, repulsive forces are generated to mitigate the overlap. The repulsive forces act on the centroid points  $c_i$  and  $c_j$  of the sensor, respectively. When the Euclidean distance between the sensors is greater than or equal to twice the sensing radius, the nodes do not affect each other, and the repulsion is 0. When the virtual negative centroid  $f_k$  is covered by the neighbor node, mark  $f_k = 0$ , indicating that the virtual negative centroid  $f_k$  has been covered and does not generate gravity; when the virtual negative centroid  $f_k$  is not covered by the neighbor node, mark  $f_k = 1$ , indicating that the virtual negative centroid  $f_k$  generates gravity on the sensor node  $f_k$ . The force analysis of the virtual force model is as follows:

$$\text{Repulsion model: } \vec{F}_{ij} = \begin{cases} \left( \sum_{j=1}^m \frac{K_R}{D_{ij}^2}, \alpha_{ij} \right), & \text{if } D_{ij} < 2r \\ \vec{0}, & \text{otherwise} \end{cases} \tag{4}$$

$$\text{Gravity model: } \vec{F}_{ik} = \begin{cases} \left( \sum_{k=1}^{f_{k\_max}} \frac{1}{D_{ik}^2}, \alpha_{ik} \right), & \text{if } f_k = 1 \\ \vec{0}, & \text{otherwise} \end{cases} \tag{5}$$

where  $D_{ij}$  denotes the Euclidean distance between the centroid point  $c_i$  and the centroid point  $c_j$ ;  $D_{ik}$  represents the Euclidean distance between the virtual negative centroid  $f_k$  of the centroid point  $c_i$  and the sensor node  $s_i$ ;  $K_R$  indicates the virtual repulsion coefficient ( $K_R = 1$ );  $\alpha_{ik}$  stands for the direction of gravity (from the centroid point  $c_j$  to the virtual negative centroid  $f_k$ );  $\alpha_{ij}$  represents the unit vector, indicating the direction of repulsion (from the center of mass point  $c_j$  to the center of mass point  $c_i$ ); and  $f_{k\_max}$  stands for the maximum number of virtual negative centroids.

In the context of sensor networks, the adjustment of sensing directions in sensor nodes is influenced not only by the virtual repulsion from neighboring nodes, but also by the virtual attraction generated by uncovered virtual negative centroid points. This combined force effectively reduces coverage overlap and blind areas in sensor networks. The magnitude of the force experienced by a sensor node  $s_i$ , which perceives the rotation of the sensing direction, can be expressed as follows (6):

$$\vec{F}_i = \sum_{j=1, j \neq i}^m \vec{F}_{ij} + \sum_{k=1}^{f_{k\_max}} \vec{F}_{ik} \tag{6}$$

The rotational motion of a directional sensor node in its sensing direction can be considered as circular motion, with the centroid point as the center and the sensing radius as the radius. The repulsive force from the neighbor node  $s_j$  and the gravitational force from the virtual negative centroid  $f_k$  of the node  $s_i$  can be decomposed into component forces along the tangent direction and the force parallel to the sensing direction of the node. Since the position of the node  $s_i$  remains unchanged, the force generated by the component force parallel to the sensing direction of the node during rotation in the direction of the node is zero. Therefore, the force experienced by the directional sensor node during movement in its sensing direction is the component force of the resultant force of the sensor node along the tangent direction. The force analysis of the directed sensor node  $s_i$  is shown in Figure 4.

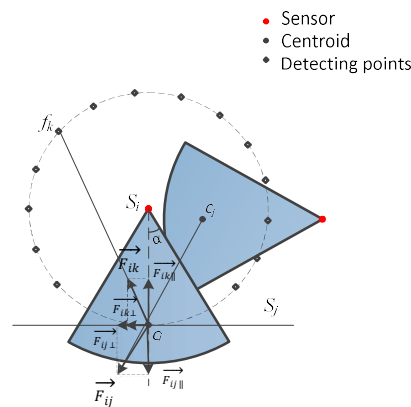


Figure 4. Force analysis of split virtual negative centroid.

#### 4. Coverage Enhancement Algorithm for Directed Sensor Networks under the Synergy of Virtual Force and Particle Swarm Optimization

Particle swarm optimization (PSO) is a global optimization algorithm in the field of swarm intelligence optimization algorithms. It possesses advantages such as fast convergence and simple calculation and has found extensive applications in coverage algorithms for directional sensor networks. In this study, the coverage enhancement algorithm for a directional sensor network, based on particle swarm optimization, was combined with the coverage enhancement algorithm for a directional sensor network utilizing segmented virtual negative centroids. The resulting optimization mechanism maximized the coverage optimization algorithm for directional sensor networks, incorporating virtual force and particle swarm optimization.

##### 4.1. Coverage of Directed Sensor Networks Based on Particle Swarm Optimization Algorithm

Assuming an initial random deployment of  $D$  sensors and  $S$  particles, where particle  $i$  represents the distribution of  $D$  sensors in the target area, the particles are influenced by the historical optimal positions of individuals (p best) and groups (g best) during motion. Through a generation-by-generation search, the optimal solution is obtained. The fitness of particle  $i$  is defined as  $f_i = C(x_{i1}, x_{i2}, \dots, x_{id})$ , which is the coverage of the target area when the perception angle of the  $N$  sensors of particle  $i$  is  $(x_{i1}, x_{i2}, \dots, x_{id})$ . It is assumed

that the initial angle of the particle is  $x_{id}^t = (x_{i1}^t, x_{i2}^t, \dots, x_{id}^t)$ ; the angle adjustment is  $v_{id}^t = (v_{i1}^t, v_{i2}^t, \dots, v_{id}^t)$ ; in a particle swarm of size  $N$ , particle  $i$  will update its velocity and position according to the following formula:

$$v_{id}^{t+1} = wv_{id}^t + c_1r_1(p_{id}^t - x_{id}^t) + c_2r_2(p_{gd}^t - x_{id}^t) \tag{7}$$

$$x_{id}^{t+1} = x_{id}^t + v_{id}^{t+1} \tag{8}$$

The optimal position of individual history is  $p_{id}^t = (p_{i1}^t, p_{i2}^t, \dots, p_{id}^t)$ ; the global optimal position is  $p_{gd}^t = (p_{g1}^t, p_{g2}^t, \dots, p_{gd}^t)$ . Therefore, the updated formula for angle adjustment and the perception angle of particle flight is as follows:

$$w = w_{max} - (w_{max} - w_{min}) * t / T_{max} \tag{9}$$

Here,  $1 \leq d \leq D$ ;  $1 \leq i \leq M$ ;  $w$  indicates the inertia weight, and its size determines the memory degree of the particle to the current velocity;  $c_1, c_2$  represent learning factors;  $r_1, r_2$  express random numbers between 0 and 1;  $w_{max}$  signifies the maximum inertia weight;  $w_{min}$  stands for the minimum inertia weight; and  $T_{max}$  pertains to the maximum number of iterations.

#### 4.2. Coverage Optimization Algorithm for Directed Sensor Networks under the Synergy of Virtual Force and Particle Swarm Optimization

According to the analysis conducted using the virtual force model, the virtual force experienced by each individual node in the sensor network was determined for a specific deployment scenario. By referring to Equation, it is evident that the angle of rotation for each node remains fixed [14]. Therefore, the coverage result derived from the virtual force model is inherently unique, thereby predisposing the network to suboptimal regions and thus impeding its coverage enhancement potential. This paper proposes a novel approach to optimize the coverage of directional sensor networks by combining the principles of virtual negative centroids and particle swarm optimization. Notably, a combined effect is observed when integrating the concepts of virtual force and particle swarm optimization. The proposed methodology involves utilizing the virtual force model to compute the resultant force acting upon each sensor node. Subsequently, the angular adjustment of particles in the solution space is calculated. Through the combined influence of the virtual resultant force and the angular adjustment of particles, the sensing direction of each sensor node is effectively modified. The flight update formula for particle I is expressed as follows:

$$v_{ij}^{t+1} = wv_{ij}^t + c_1r_1(p_{ij}^t - \theta_{ij}^t) + c_2r_2(p_{gj}^t - \theta_{ij}^t) \tag{10}$$

$$f^{t+1} = c_3r_3\delta_{ij}(t) \tag{11}$$

$$\theta_{ij}^{t+1} = \theta_{ij}^t + v_{ij}^{t+1} + f^{t+1} \tag{12}$$

$$k_i = \frac{\arctan F_i}{\pi/2} \tag{13}$$

$$\delta_{ij}(t) = k_i * \delta_{max} \tag{14}$$

Here, the inertia weight is  $w$ ;  $c_1, c_2, c_3$  represent learning factors;  $r_1, r_2, r_3$  denote random numbers between 0 and 1;  $F_i$  expresses the virtual resultant force of sensor node  $i$ ; the value of  $\delta_{max}$  is  $5^\circ$ ; and  $v_{ij}^t$  indicates the angle adjustment of the  $j$ -dimensional sensor node of the  $i$ -th particle in the  $t$ -th iteration.  $\theta_{ij}^t$  expresses the sensing direction of the  $j$ -dimensional sensor node of the  $i$ -th particle in the  $t$ -th iteration;  $p_{ij}^t$  stands for the individual

optimal position of the  $j$ -dimensional sensor node of the  $i$ -th particle in the  $t$ -th iteration;  $p_{gj}^t$  illustrates the global optimal position of the sensor node in the  $t$ -th iteration.

The role of inertia weight in the PSO optimization algorithm is of paramount importance. The linear decrease in inertia weight endows particles with a positive performance in global search at the onset of the search process, swiftly identifies the global optimal region, and confers favorable local search capability in the later stages. This collective behavior enables the accurate identification of the global optimal solution. However, due to its linear decrease characteristics, escaping from local optima becomes challenging once the algorithm reaches a local extreme point during the later stages. Building upon the aforementioned analysis, this study proposes an inertia weight strategy based on the properties of the cosine function, which divides the inertia weight into two stages: an increasing stage (the first stage) and a decreasing stage (the second stage). The enhanced inertia weight strategy is outlined as follows:

$$w = \begin{cases} \{w_{max} - (w_{max} - w_{min})\cos\left(\frac{\pi t}{T_{max}}\right)\}, & 0 \leq \frac{t}{T_{max}} \leq 0.5 \\ \{w_{max} + (w_{max} - w_{min})\cos\left(\frac{\pi t}{T_{max}}\right)\}, & 0.5 \leq \frac{t}{T_{max}} \leq 1 \end{cases} \quad (15)$$

Here,  $w_{max}$  represents the maximum inertia weight,  $w_{min}$  denotes the minimum inertia weight, and  $T_{max}$  expresses the maximum number of iterations.

It can be inferred from Equation (15) that, in the initial stage, the particle enhances its global optimization capability by consistently increasing the inertia weight and detecting the global optimal region. Notably, in the subsequent stage, the particle improves its local optimization capability by reducing the inertia weight to identify the global optimal solution. However, the local capability gradually strengthens during this stage, making it susceptible to falling into the local optimum and resulting in a slow convergence rate in the later evolutionary phase. To address this issue, Gaussian disturbance is introduced during the particle update in the second stage, thereby augmenting its ability to escape local optimization and preventing premature convergence of the algorithm. Therefore, the convergence speed and accuracy of the algorithm are enhanced. The updated formulation of the coverage optimization algorithm for directional sensor networks, under the synergistic effect of the improved virtual force and particle swarm optimization algorithm, is presented as follows:

$$\begin{cases} v_{ij}^{t+1} = wv_{ij}^t + c_1r_1(p_{ij}^t - \theta_{ij}^t) + c_2r_2(p_{gj}^t - \theta_{ij}^t), & 0 \leq \frac{t}{T_{max}} \leq 0.5 \\ v_{ij}^{t+1} = wv_{ij}^t + c_1r_1(p_{ij}^t + r_2gauss_{ij}^t - \theta_{ij}^t) + c_2r_3(p_{gj}^t - \theta_{ij}^t), & 0.5 \leq \frac{t}{T_{max}} \leq 1 \end{cases} \quad (16)$$

$$f^{t+1} = c_3r_3\delta_{ij}(t) \quad (17)$$

$$\theta_{ij}^{t+1} = \theta_{ij}^t + v_{ij}^{t+1} + f^{t+1} \quad (18)$$

$$gauss_{ij}^t = r_4gaussian(\mu, \sigma^2) \quad (19)$$

Here,  $w$  represents the inertia weight;  $c_1$ ,  $c_2$  denote learning factors;  $r_1$ ,  $r_2$ ,  $r_3$ ,  $r_4$  indicate random numbers between 0 and 1;  $v_{ij}^t$  expresses the velocity of particle  $i$  in the  $t$ -th iteration;  $p_{ij}^t$  conveys the historical optimal position of the particle  $i$  in the  $t$ -th iteration;  $p_{gj}^t$  stands for the global optimal position of the particle  $i$  in the  $t$ -th iteration;  $p_{gj}^t$  refers to the Gaussian disturbance generated by particle  $i$  in the  $t$ -th iteration;  $\mu$  pertains to the mean; and  $\sigma^2$  illustrates the variance. The specific steps of the algorithm in this paper are shown in Figure 5.



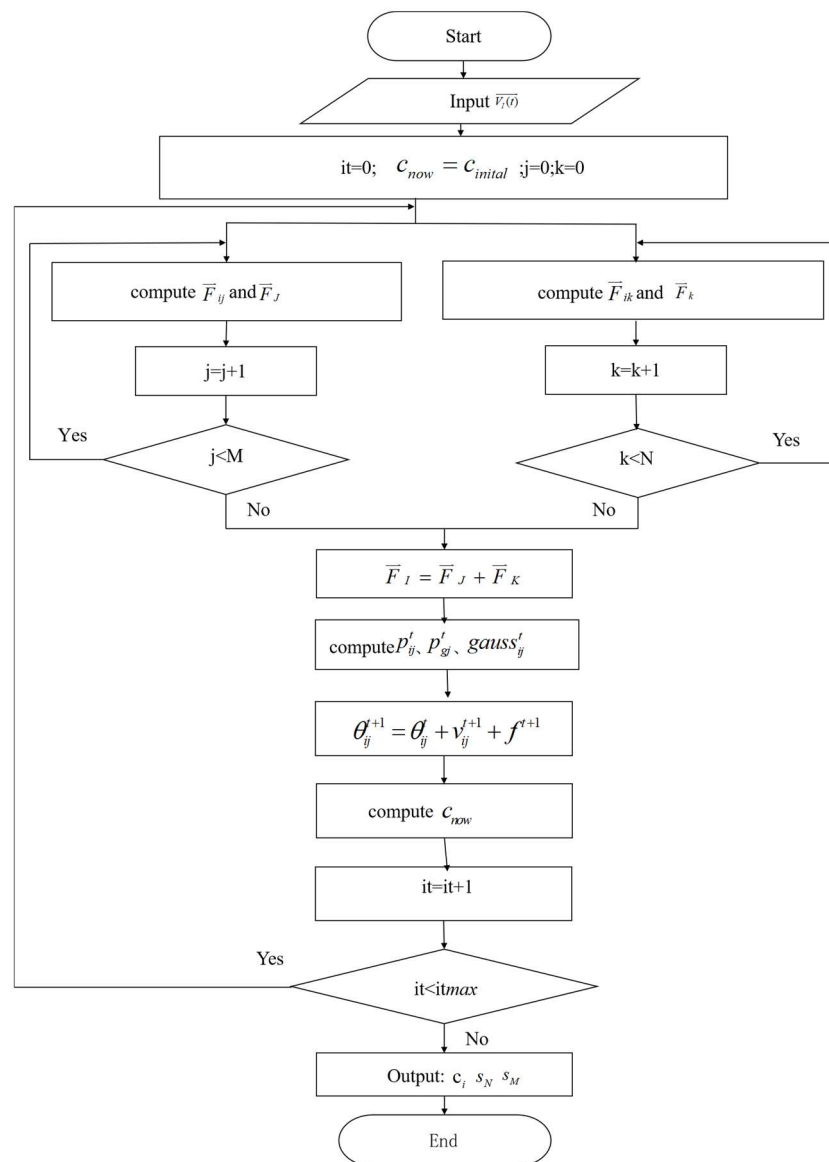


Figure 5. Algorithm step diagram.

Here, it is the initial number of iterations,  $c_{now} = c_{initial}$  represents the initial coverage rate,  $c_i$  denotes the centroid point,  $s_N$  indicates the virtual negative centroid set,  $s_M$  depicts the neighbor node set,  $M$  conveys the number of neighbor nodes, and  $N$  expresses the number of virtual negative centroids.  $\vec{F}_{ij}$  is generated by the neighbor node  $s_j$  to the calculated node  $s_i$ ,  $\vec{F}_J$  stands for virtual repulsion vector sum,  $\vec{F}_{ik}$  illustrates the virtual gravity,  $\vec{F}_I$  stands for the sum force of  $s_i$ ,  $p_{ij}^t$  signifies the optimal particle position of the population, and  $gauss_{ij}^t$  expresses the Gaussian disturbance value of the calculated particles.

## 5. Algorithm Simulation and Result Analysis

### 5.1. Experimental Results and Analysis

#### 5.1.1. Experimental Environment and Parameter Setting

An Intel (R) Core (TM) i5-7200U (2.5 GHz) CPU, with 4 GB of memory, running on a 64-bit Windows 10 operating system was employed in the experimental setup. The algorithm was validated using C++ programming and the control variable method. The experimental section consists of two parts: firstly, the experimental results and analysis of the algorithm proposed in this paper; secondly, a comparison of the algorithm with similar

approaches to verify its effectiveness. The parameters used in the experimental setup are presented in Tables 1 and 2.

**Table 1.** Scene parameters.

Parameter	Region Area	Number of Logistics Nodes N	Sensing Radius r	Perception Angle $\alpha$
value	$500 \times 500\text{m}^2$	106	60 m	$45^\circ$

**Table 2.** Algorithm parameters.

Parameter	Population Size	Iterations	$w_{\max}$	$w_{\min}$	$c_1$	$c_2$	$c_3$
value	40	50	0.9	0.4	0.729	0.729	1.414

### 5.1.2. Diagram of Experimental Results and Comparative Analysis

#### 1. Coverage algorithm for directional sensor networks with segmented virtual negative centroid.

For this paper, the sensing angles of directional sensor nodes were partitioned into n (n = 1, 2, 3, 4, 5, 6, 7, 8, 9, 10, and 15) equal segments to establish the virtual negative centroid, while considering various radii, sensing angles, and target areas. The optimization of sensor network coverage yielded diverse results based on different preconditions and n values, as elaborated in Table 3.

**Table 3.** Coverage under different parameters (%).

	Initial Value	VF	One	Two	Three	Four	Five	Six	Seven	Eight	Nine	Ten	Fifteen	
r = 50	65.04	71.8	74.76	74.96	75.36	75.6	75.16	75.08	75.56	74.92	75.48	74.96	75.64	3.84
r = 60	66	71.96	73.12	73.4	74.2	73.88	74.24	74.44	73.84	73.52	74.72	73.48	74.4	2.24
r = 70	68.96	72.28	73.2	73.24	73.88	73.56	73.96	73.76	73.64	73.8	73.92	74.04	73.84	1.76
$\alpha = 30$	68.44	76.48	77.76	78.56	78.28	78.12	78.4	78.4	77.56	74.72	76.68	78.08	77.88	2.08
$\alpha = 45$	65	70.44	71.88	72.44	72.84	72.52	72.6	72.52	72.68	72.64	72.68	72.72	72.52	2.4
$\alpha = 60$	69.2	72.36	72.64	72.96	73.32	73.6	73.68	73.68	74.44	74	74.76	73.96	74.08	2.4
s = $400 \times 400\text{m}^2$	66.69	72.75	72.94	73.12	74.06	73.44	74.13	74.31	74.94	75	74.56	75.06	74.75	2.31
S = $500 \times 500\text{m}^2$	64.72	70.2	71.76	71.96	72.96	72.72	73.52	73.56	73.8	74.24	73.56	74.12	73.64	4.04
S = $600 \times 600\text{m}^2$	65.14	70.56	74.44	74.69	75.36	75.14	75.31	75.61	75.25	74.89	75.42	75.14	75.67	5.11
S = $700 \times 700\text{m}^2$	66.22	71.5	75.84	75.69	76.22	76	76.33	76.29	76.1	75.55	76.2	75.16	76.27	4.83

As depicted in Table 4, when compared to the VF algorithm proposed in the reference, the coverage algorithm for directional sensor networks presented in this paper exhibited notable enhancements. Specifically, the directional sensor was divided into multiple equal segments, and the number of virtual negative centroids established in the coverage blind area was increased. Therefore, the gravitational influence exerted on the coverage blind area was effectively enhanced, thereby guiding the sensor nodes to swiftly transition from the coverage overlapping area to the coverage blind area. This approach significantly improved the coverage of the sensor network. Regardless of the partitioning scheme, the achieved coverage value surpassed that optimized by the VF algorithm. For instance, when  $S = 600 \times 600\text{m}^2$ , the coverage value obtained from this algorithm exceeded that of the VF algorithm by 5.11%. Moreover, when  $r = 60$ ,  $\alpha = 45$ , and  $S = 500 \times 500\text{m}^2$ , three distinct initialization scenarios with identical parameters were considered, and the directional sensor was subjected to multi-initialization. According to Table 4, when the number of directional sensors equaled or exceeded five, the optimal coverage ratio reached 80%.

**Table 4.** Comparative analysis of data.

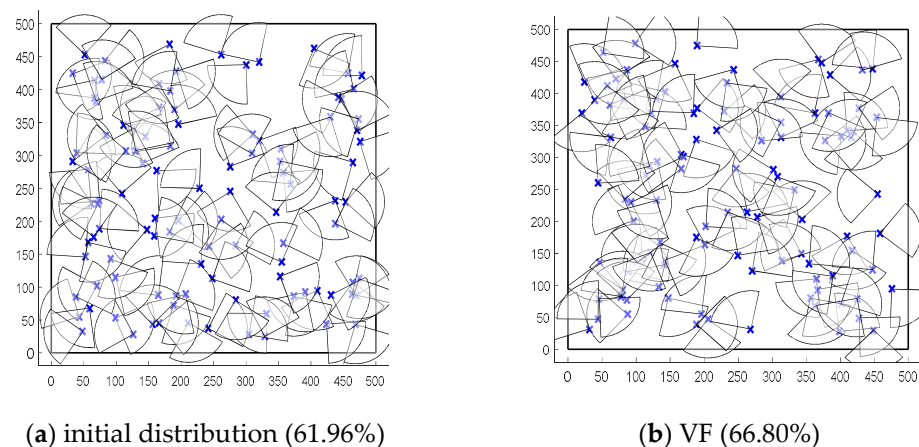
Algorithm	Mean Coverage Rate	Maximum Coverage
Algorithm in this paper	80.61%	84.2%
LAASD	75.5%	-
VF-PSO	75%	78%
OSRCEA	73.8%	-
PSO	70.13%	70.52%
VF	64.64%	64.64%

## 2. Coverage algorithm of directional sensor networks under the synergistic effect of virtual force and particle swarm optimization.

Regarding the designated area of  $500 \times 500\text{m}^2$ , as per the computational methodology expounded in reference [24], in order to achieve a coverage rate surpassing 70%, it is necessary to establish the initial deployment of sensor nodes in a random manner, with a count of 106. The sensing radius of each sensor should be set at 60 m, while particle  $\alpha = 45^\circ$ , and the population size should be set at 40. The positional coordinates and orientation angles of the randomly deployed sensor nodes are depicted in Figure 6a, with the initial coverage rate being estimated at 61.96%, according to Formula (1). Subsequently, the VF, 3-MD-VF, and VF-PSO algorithms, as well as the algorithm devised in this study, were executed independently for 30 iterations, utilizing the aforementioned initial value. The optimal coverage rates obtained from the four algorithms were 66.80%, 69.68%, 73.58%, and 84.2%, respectively. The corresponding coverage topologies are represented in Figure 6b–e.

In comparison to the initial coverage rate of 61.96%, the VF algorithm exhibited an enhancement, elevating the coverage rate to 66.80%. In addition, our superior 3-MD-VF algorithm demonstrated a further increase in the coverage rate, reaching 69.68%, which was 2.82% higher than that achieved by the VF algorithm. Intriguingly, the VF-PSO algorithm yielded a coverage rate of 73.58%, while our proposed algorithm achieved a remarkable coverage rate of 84.2%, surpassing the initial coverage rate by 22.24%. Therefore, the algorithm presented in this paper outperformed the other algorithms in terms of optimizing the coverage effect for sensor networks.

To evaluate the optimization performance of the algorithm across various initial deployments, ten random node deployments were generated, yielding corresponding initial coverage rates of 59.88%, 61.64%, 61.96%, 62.2%, 63.36%, 63.96%, 64.32%, 64.56%, 65.05%, and 65.24%, respectively. For each initial deployment, separate experiments were conducted, and the coverage curve depicted the average coverage achieved by each algorithm over ten iterations, as illustrated in Figure 7.

**Figure 6.** Cont.

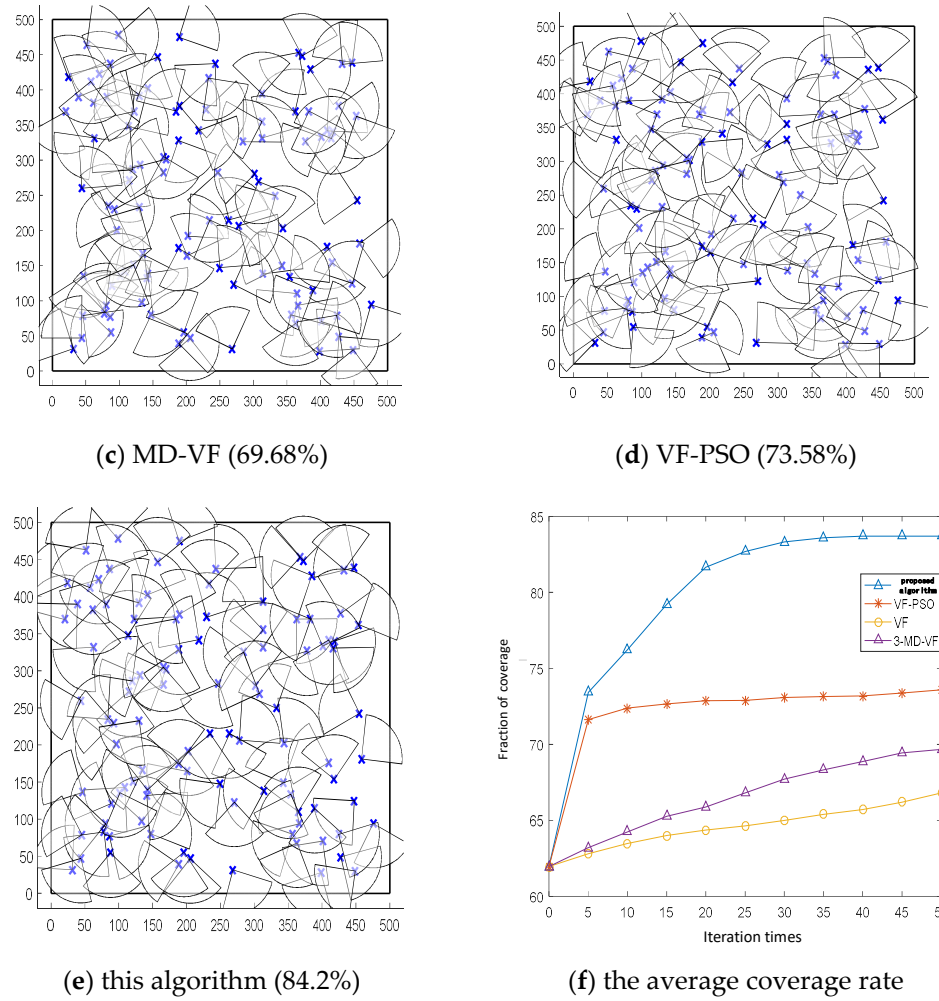


Figure 6. Distribution and coverage curve of sensor experimental results.

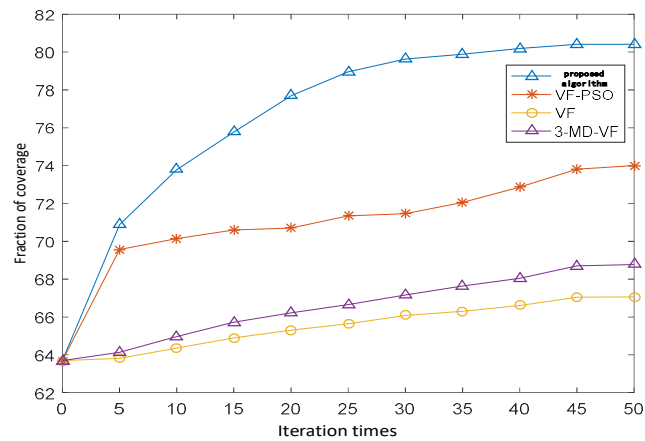


Figure 7. Ten-deployment (average) coverage curve.

Subsequent to the 10 random initial deployments, the VF algorithm, the 3-MD-VF algorithm, the VF-PSO algorithm, and our algorithm were subjected to testing, resulting in coverage rates of 67.24%, 68.77%, 73.99%, and 80.41%, respectively. Figure 6, displaying the graph of the coverage across the ten deployments (average), reveals that our algorithm outperformed the VF algorithm, 3-MD-VF algorithm, and VF-PSO algorithm in terms of coverage effectiveness for different initial deployments. This finding substantiates the robust adaptability of our algorithm to diverse deployment scenarios.

### 5.2. Comparison between Our Algorithm and Other Similar Algorithms

#### 5.2.1. Experimental Parameter Settings

Compared with LAASD [18], VF-PSO [25], OSRCEA [26], PSO [23], and VF [27], the number of nodes in the experimental parameter setting was 100, and the remaining parameters were consistent with Tables 1 and 2.

#### 5.2.2. Analysis of Experimental Results

To further verify the effectiveness of the algorithm, a comparison was made between our algorithm and the LAASD, VF-PSO, OSRCEA, PSO, and VF algorithms, with a focus on their average coverage and maximum coverage. The results of this analysis are presented in Table 4.

As illustrated in Table 4, the mean coverage rate of the VF algorithm was found to be 64.64%. Subsequently, through optimization, the PSO algorithm achieved a coverage rate of 70.13%. Following the optimization of the OSRCEA algorithm, its coverage rate increased to 73.8%. Moreover, the VF-PSO algorithm led to a coverage rate of 75% after optimization, while the LAASD algorithm achieved a coverage rate of 75.5% after optimization. Finally, our algorithm resulted in an average coverage rate of 80.16% for the network, with a maximum coverage rate of 84.2%. These findings suggest that the proposed coverage optimization algorithm for directional sensor networks, which combines virtual force and particle swarm optimization, outperforms other algorithms in terms of achieving a larger coverage area and a desirable coverage effect.

### 5.3. Influence of Different Parameters on Coverage Rate

In this experiment, the researchers employed the control variable method, with the number of nodes, perception radius, and perception angle serving as the controlled variables, while keeping the remaining parameters constant. Subsequently, the algorithm developed in this study was compared with the VFPSO, MD-VF, and VF algorithms. Through a series of comparative experiments, the relationship between coverage and the number of nodes, perception radius, and perception angle was analyzed. The monitoring area for the experiment was  $8.500 \times 500\text{m}^2$ , with the number of nodes set at 50, 70, 90, 110, and 130; the sensing radius at 40, 50, 60, 70, and 80; and the sensing angle at  $30^\circ$ ,  $40^\circ$ ,  $50^\circ$ ,  $60^\circ$ , and  $70^\circ$ . The experimental results are presented in Figure 8.

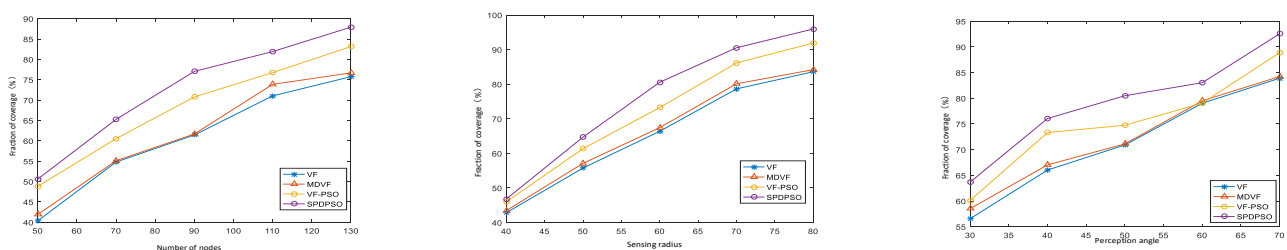


**Figure 8.** Influence of number of nodes, perception radius, and perception angle on coverage.

It is evident from Figure 7 that as the number of nodes increases, the coverage rate also exhibits an upward trend. However, excessive node deployment leads to a significant overlap in coverage, resulting in a surplus of redundant nodes and therefore impeding coverage growth. Specifically, when  $N = 130$ , the proposed algorithm demonstrates improvements of 4.77, 11.24, and 12.16 over the VF-PSO algorithm, MD-VF algorithm, and VF algorithm, respectively. From the coverage distribution map of the sensing radius from 40 to 80, it can be seen that the coverage of the three algorithms increases with the increase in the sensing radius  $R$ . Notably, when  $R = 80$ , the proposed algorithm outperforms the VF-PSO algorithm, MD-VF algorithm, and VF algorithm by 4.06, 11.76, and 12.36, respectively. In addition, for the perception angle  $\alpha$ , when gradually increasing from  $30^\circ$  to  $70^\circ$ , the coverage increases with the increase in the perception angle  $\alpha$ . Specifically, when  $\alpha = 70^\circ$ ,

the algorithm is improved by 3.69, 8.33, and 8.65, respectively, compared with the VF-PSO algorithm, MDVF algorithm, and VF algorithm.

The aforementioned analysis suggests that the integration of the virtual force model and particle swarm optimization algorithm not only overcomes the limitations associated with virtual force optimization results but also expedites particle optimization. This integration effectively guides sensor nodes towards the optimal direction, thereby minimizing coverage overlap and blind areas. Therefore, sensor networks can promptly detect the global optimal solution.

#### 5.4. The Universality Analysis of This Model

The analysis in this study primarily relies on directional mobile sensors. These sensors possess the capability to autonomously perceive and collect data in the designated detection area, subsequently transmitting the collected data. The sensor system primarily comprises a sensor module, a data processing module, a wireless communication module, and an energy supply module, as depicted in Figure 9.

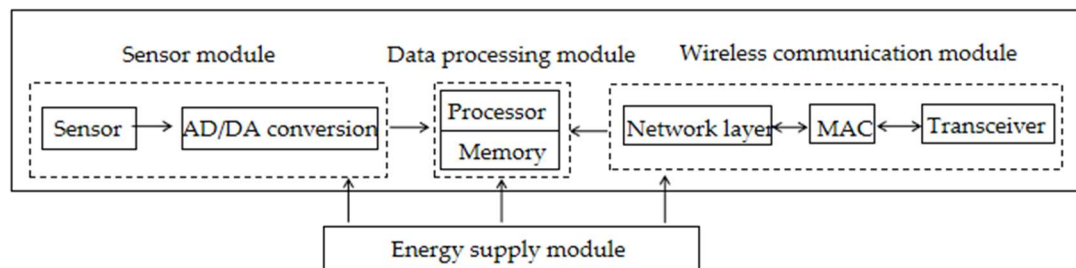


**Figure 9.** Sensor node structure diagram.

The sensor module assumes responsibility for the perception and collection of data in the monitoring area. Subsequently, the collected data undergo conversion through an A/D converter before being transmitted to the data processing module. The data processing module is tasked with storing and processing the converted data, while also coordinating the various modules in the sensor node. The wireless communication module is responsible for managing the exchange, reception, transmission, and forwarding of information, serving as a crucial “bridge” between the two nodes. Finally, the energy supply module ensures the provision of sufficient energy to sustain the operation of each module in the sensor node. Therefore, directional sensors are generally capable of fulfilling the aforementioned tasks.

The detection of common regions is not limited to rectangular shapes; rather, it comprises irregular regions as well. In such cases, the irregular region can be converted into a minimum bounding rectangle that encapsulates it. By employing the algorithm presented in this study to validate the rectangular region, it becomes evident that the irregular region, being a subset of the rectangular region, adheres to the algorithm’s requirements. Thus, this paper successfully verifies the algorithm’s applicability to both rectangular and irregular regions.

## 6. Conclusions

Under the context of the coverage optimization problem encountered in directional sensor networks, an algorithm for coverage optimization is proposed in this study. The algorithm leverages the cooperative efforts of a virtual force model and a particle swarm optimization algorithm. Notably, the algorithm enhances the conventional virtual force model by refining the methodology for establishing the virtual negative centroid and adjusting the optimization impact of coverage blind areas on the network. Subsequently, the virtual force model and particle swarm optimization algorithm are synergistically employed to regulate the orientation of sensor nodes. In the particle optimization process, improvements are made to the inertia weight strategy to prevent particles from converging towards

local optima. Additionally, the introduction of Gaussian disturbance expedites particle convergence, facilitating the rapid attainment of an optimal distribution across the entire network. The experimental findings demonstrate that the coverage optimization algorithm, which integrates virtual force and particle swarm optimization, achieves superior coverage performance, thereby substantiating its efficacy. This study employed a series of simulation experiments to evaluate the algorithm. Initially, the sensor network exhibited a coverage of 31.04%. However, following the algorithm's optimization, the average coverage of the network increased to 80.16%, with a maximum coverage of 84.2%, thereby confirming the algorithm's effectiveness.

The S-VFPSO algorithm, as proposed in the confines of this paper, serves the purpose of adjusting the sensing direction of nodes. Additionally, the enhanced particle swarm optimization algorithm is employed to optimize the positioning of said nodes in the network. Through the combined influence of these two algorithms, the nodes in the sensor network are guided towards attaining an optimal distribution throughout the network, thereby enhancing the network's effective coverage. As the application scenarios pertaining to sensor networks grow increasingly complex, the exploration of coverage optimization in three-dimensional space for directional mobile sensor networks emerges as a pivotal area of research. Sensor nodes in such networks possess the capacity for directional adjustability and mobility, albeit at the cost of significant energy expenditure. In addition, the multifaceted functionalities of these nodes necessitate higher configurations. Considering the widespread implementation of directional mobile sensor networks, it is necessary to delve into various key technologies, including but not limited to energy consumption reduction, network lifespan extension, and topology control; these issues warrant in-depth study.

**Author Contributions:** Conceptualization, L.Z.; Resources, L.L.; Methodology, Q.L.; Validation, Y.L.; Investigation, H.T. and D.Z.; Supervision, X.M. All authors have read and agreed to the published version of the manuscript.

**Funding:** This study was supported by the National Natural Science Foundation of China and the Department of Science and Technology of Shaanxi Province, No.52175186,2023-ZDLGY-14.

**Data Availability Statement:** Not applicable.

**Conflicts of Interest:** The authors declare no conflict of interest.

## References

1. Guvensan, M.A.; Yavuz, A.G. On coverage issues in directional sensor networks: A survey. *Ad Hoc Netw.* **2011**, *9*, 1238–1255. [[CrossRef](#)]
2. Tian, X.; He, J.; Guo, M.; Liu, G.; Zhu, Y. Mobile charging and data collection strategies in wireless sensor networks. *J. Instrum.* **2018**, *39*, 216–224.
3. Li, M.; Hu, J. Coverage algorithm for mobile heterogeneous wireless sensor networks under complex conditions. *Sens. Microsyst.* **2019**, *38*, 124–127+132.
4. Liu, C.; Zhao, Z.; Qu, W.; Qiu, T.; Sangaiah, A.K. A distributed node deployment algorithm for underwater wireless sensor networks based on virtual forces. *J. Syst. Archit.* **2019**, *97*, 9–19. [[CrossRef](#)]
5. Li, F.X.; Islam, A.A.; Jaroo, A.S.; Hamid, H.; Jalali, J.; Sammartino, M. Urban highway bridge structure health assessments using wireless sensor network. In Proceedings of the 2015 IEEE Topical Conference on Wireless Sensors and Sensor Networks (WiSNet), San Diego, CA, USA, 25–28 January 2015; pp. 75–77.
6. Sun, S.Z.; Xiang, Y.; Dang, X.Y. Research on FBG flow and temperature composite sensor based on the PSO decoupling algorithm. *Chin. J. Sci. Instrum.* **2022**, *43*, 2–10.
7. Varposhti, M.; Hakami, V.; Dehghan, M. Distributed coverage in mobile sensor networks without location information. *Auton. Robot.* **2020**, *44*, 627–645. [[CrossRef](#)]
8. Cheng, S.; Yuan, F. Coverage control for mobile sensor networks with limited communication ranges on a circle. *Automatica* **2018**, *92*, 155–161.
9. Zhang, H.D.; Shi, W.R.; Yang, L. Study on equilibrium of particle-based coverage control for mobile sensor network. *Chin. J. Sci. Instrum.* **2016**, *37*, 1049–1057.
10. Thandapani, P.; Arunachalam, M.; Sundarraj, D. An energy-efficient clustering and multipath routing for mobile wireless sensor network using game theory. *Int. J. Commun. Syst.* **2020**, *33*, e4336. [[CrossRef](#)]

11. Wu, Y.; Liu, K.; Chen, B.; Li, F.; Yao, J. Image reconstruction for electrical impedance tomography using radial basis function neural network optimized with adaptive particle swarm optimization algorithm. *Chin. J. Sci. Instrum.* **2020**, *41*, 240–249.
12. Si, P.; Wu, C.; Zhang, Y.; Chu, H.; Teng, H. Probabilistic coverage in directional sensor networks. *Wirel. Netw.* **2019**, *25*, 355–365. [[CrossRef](#)]
13. Years, I.R. Distributed Voronoi-Based Self-Redeployment for Coverage Enhancement in a Mobile Directional Sensor Network. *Int. J. Distrib. Sens. Netw.* **2013**, *9*, 165498.
14. Varposhti, M.; Saleh, P.; Afzal, S.; Dehghan, M. Distributed area coverage in mobile directional sensor networks. In Proceedings of the 2016 8th International Symposium on Telecommunications (IST), Tehran, Iran, 27–28 September 2016; pp. 18–23.
15. Fan, X.G.; Wang, H.; Hao, X. Coverage Enhancement Algorithm for Directed Sensor Networks. *Chin. J. Sci. Instrum.* **2017**, *38*, 368–377.
16. Peng, S.; Xiong, Y. An Area Coverage and Energy Consumption Optimization Approach Based on Improved Adaptive Particle Swarm Optimization for Directional Sensor Networks. *Sensors* **2019**, *19*, 1192. [[CrossRef](#)]
17. Esmaeilzadeh, R.; Abbaspour, M. Optimum Temporal Coverage with Rotating Directional Sensors. *Wirel. Pers. Commun.* **2019**, *105*, 369–386. [[CrossRef](#)]
18. Liu, Z.; Ouyang, Z. A Learning Automata-based Algorithm for Area Coverage Problem in Directional Sensor Networks. *KSII Trans. Internet Inf. Syst.* **2017**, *10*, 4807–4822.
19. Zhang, G.; You, S.; Ren, J.; Li, D.; Wang, L. Local Coverage Optimization Strategy Based on Voronoi for Directional Sensor Networks. *Sensors* **2016**, *16*, 2183. [[CrossRef](#)]
20. Yuen, K.; Kuok, S. Efficient Bayesian sensor placement algorithm for structural identification: A general approach for multi-type sensory systems. *Earthq. Eng. Struct. Dyn.* **2015**, *44*, 757–774. [[CrossRef](#)]
21. Jiang, Y.B.; Wang, W.; He, C.L. Sub-regional Dynamic Optimization Algorithm for Path Coverage of Single Target. *Comput. Sci.* **2019**, *46* (Suppl. 2), 369–375.
22. Zhang, J.W.; Wang, Y. Strong barrier coverage algorithm for directional sensor network. *J. Electron. Meas. Instrum.* **2017**, *31*, 83–91.
23. Duan, S.; Shi, Q.; Wu, J. Multimodal Sensors and ML-Based Data Fusion for Advanced Robots. *Adv. Intell. Syst.* **2022**, *4*, 2200213. [[CrossRef](#)]
24. Wang, C.; Mao, J.; Fu, L.; Guo, N.; Qu, W. Coverage optimization algorithm for three-dimensional directional heterogeneous sensor network. *J. Comput. Appl.* **2016**, *36*, 2362–2366+2373.
25. Yang, Y.F. *Research on Coverage Enhancement Algorithm of Multimedia Sensor Networks Based on 3D Perceptual Model*; Northeastern University: Shenyang, China, 2015.
26. Fan, X.G.; Wang, H.; Zhang, Z.J. A Virtual Force-Directed Particle Swarm Optimization for Coverage Enhancing in directional sensor networks. *Chin. J. Sens. Actuators* **2015**, *28*, 1720–1726.
27. Jiang, Y.B.; Mei, J.D.; Wang, N.H. Directional Sensor Network Coverage Optimization Algorithm with Modify Virtual Force k. *J. Chin. Comput. Syst.* **2018**, *39*, 457–462.

**Disclaimer/Publisher's Note:** The statements, opinions and data contained in all publications are solely those of the individual author(s) and contributor(s) and not of MDPI and/or the editor(s). MDPI and/or the editor(s) disclaim responsibility for any injury to people or property resulting from any ideas, methods, instructions or products referred to in the content.